AN APPROACH TO TREE DAYLIGHTING SIMULATION USING MODELS BASED ON SOLAR CONTROL SYSTEMS

Ayelén Villalba[1,2], Andrea Pattini[1], Érica Correa[1]
[1]Human Environment and Housing Laboratory - Institute of Human, Social and Enviormental Science (INCIHUSA)-(CCT Mendoza - CONICET)
C.C.131 C.P. 5500 – Mendoza. e-mail: avillalba@mendoza-conicet.gob.ar
[2]Pg Postgraduate MAVILE, Faculty of Sciences and Technology, National University of Tucumán.

ABSTRACT

In oasis cities urban forest shades the lower level facades of buildings. It is thus crucial to analyze the distributional patterns of sun radiation produced by trees on facades. On the assumption that lighting behavior of trees as sun control elements more closely resembles a louvers system rather than other frequently used solar control systems (ej. perforated obstruction), the present study seeks to verify which of these formal simplifications adjusts better to the real case. The methodology used in this study relies on simulation models generated with hemispherical images. Louvers model showed a high degree of adjustment (RMSE 9%).

INTRODUCTION

Urban forest can bring solar protection to buildings, reducing energy consumption for interior thermal conditioning due to its shade effect and the phenomena of mass and energy transference that produces the diminishing of temperature in cities. Besides, urban trees serve as a sound barrier, reduce erosion, control wind speed and mitigate pollution (Santamouris et al., 2001, Correa et al., 2012).

Added to the benefits related to energy saving, the improvement of environmental conditions and the thermal habitability of space (Ruiz et al, 2010; Correa et al, 2010); there are studies that show the remarkable predilection of people for trees. Getz (1982) explains in his works of preference that urban trees have a considerable relevance for people when choosing a residence, and informs that trees contribute significantly in the value of the property due to their aesthetical attributes, comfort associated with atenuation of solar radiation and the increase of privacy.

Afore mentioned benefits have propitiated the selection of the “oasis city” model -wide streets and intense forestation- for the urban development of arid areas (figure 1).

Regarding daylighting there are relatively few studies that analyze urban trees as sun control elements for interior spaces. Coder (1996) explains the ability of the grove for reducing glare, states that trees help to control light disperssion, light intensity as well as they modify the predominant wavelengths in the site where they are located. He also states that they block and reflect sun light and artificial light, thus diminishing ocular tension, and frame areas lit for architectonic emphasis, security and visibility (Coder, 1996).

Figure 1: Oasis city of Mendoza, reference case in this study.

Due to the mentioned effects, urban forestry needs to be analyzed as an environmental item.

In oasis cities public grove shades the lower level facades of buildings (Córica, 2009; Villalba et al., 2012). It is thus crucial to systematically analyze the distributional patterns of visible solar radiation produced by trees on facades. Furthermore the development of predictive simulation models to be used in the study of interior spaces so as to achieve energy efficiency and visual comfort is of primary importance.

In particular, for those approaches in which the use of simulation tools is required, the geometrical and optical representation becomes highly complex. Thus, it is necessary to know several characteristics of trees such as size, leaf area, leaf reflectance and distribution. Some data such as the magnitude of the grove are simple to find in bibliography, however, there are others such as leaf density and distributional patterns which are difficult to obtain (Al-Sallal, 2009). This situation becomes even more complex for the case of urban trees, whose phenology is modified by the pruning regimes, irrigation and urban morphology (Martinez, 2011).

Given this context and the complexity of the "canopy" as an element of study, it is necessary to simplify its representation without losing precision.

On the assumption that the lighting behavior of trees as sun control elements more closely resembles a louvers system with a certain degree of transparency rather than other frequently used solar control systems, such as perforated obstruction (screen panel) or elements of homogenous transmittance (textile curtain) (figure 2), the present study seeks to verify which of these formal simplifications adjusts better to the real case, by contrasting with vertical illuminance values measurements on facade in a forested street. The tree species selected for this study is a Morus alba, commonly known as mulberry.

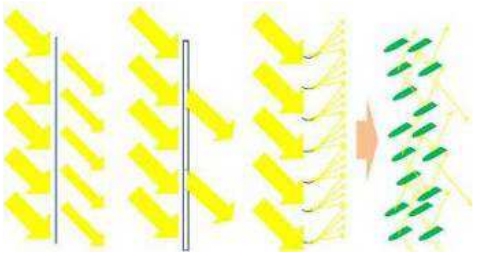

Figure 2: element of homogenous transmittance (a), system of perforated obstruction (b), louvers system (c), tree (d).

The function of trees as solar light control element will be modelled according to its similarity to three traditional solar control elements:

* multi-layered louvers system. This corresponds to what Baker (1993) calls solar filters, elements that entirely cover an opening protecting the interior from direct sun radiation.

*system of perforated obstruction, screen panel type.

*homogenous transmittance system, e.g translucent wall.

As regards to tree canopies, hemispherical photography and image analysis software constitute a fundamental tools (Al-Sallal, 2009). The use of hemispherical photography in architectural design is becoming increasingly frequent. It is used to analyze the influence of buildings and the topography in relation to radiation availability and even to analyze the influence of a window in an interior space (Al-Sallal, 2009, Rodríguez, 2012). Therefore, the methodology used in this study relies on simulation models generated with hemispherical images.

BACKGROUND

There are precedents in the Human Environment and Housing Laboratory, INCIHUSA, related to development of software for hemispherical image analysis. The SKY PIXEL (PIXEL DE CIELO) programme has been developed in DELPHI 5.0 and operates in Windows. This tool allows obtaining the sky vision factor value for a certain point through digital JPG format images (Correa et al., 2005). This tool has been employed in studies related to the availability of visible solar radiation, where daily and seasonal solar dynamic, sky vision factors and "permeabilities" are shown (Córica, 2009).

Al-Sallal (2007) determines the density of canopies with photographies in studies related to the daylighting availability of classrooms. The precision of the 3D model is kept by making the canopy density of the real trees match with the models, based on the image analysis of black pixels (leaves representation) and white pixels (sky representation).

In 2009, Al-Sallal develops a method for modeling trees in daylighting simulations using hemispherical images. The method employs high-quality hemispherical photographies which are later analyzed to calculate the visible sky area, used for the theoretical model calculations.

Campbell and Norman (1989) explain that the ellipsoidal shapes are a good approximation to the tree profile. This concept known as Ellipsoidal Leaf Angle Distribution Parameter (ELADP) was later used by Al-Sallal in his works.

If we bear in mind the phenological modifications of trees on the urban environment, it is possible to observe that in high density areas the geometry-based models are quite distant from reality.

Thus it is important to employ hemispherical images to describe the tree morphology in urban areas.

SIMULATION AND EXPERIMENT

The methodology employed in the present study is divided into five stages: acquisition and processing of hemispherical image, virtual model generation (determination of optical and geometrical characteristics), reference measurement, simulation run and statistical analysis of results.

Acquisition and processing of hemispherical image.

Vertical digital images were taken with a Nikon Coolpix 5400 camera and a Nikon FC-E9 fisheye lens. The advantage of using a Nikon lens is its close to equiangular projection. In previous studies, only a 0.3º value was found to be excluded from the digital image (Blennow, 1995). The images were captured over the frontline of the building at a level corresponding to the middle point of the canopy (figure 3). In congruence with the objective of research that seeks to determine which of the selected models reproduces more accurately the access of sunlight to the front facades in presence of street forestation.

Afterwards the images were processed with SKY PIXEL software to determine the area of the photo that corresponds with the tree and the area that represents the environment, either street, buildings or

sky (figure 4). This allows isolating the sectors corresponding to the grove.

Figure 3: hemispherical image selected.

Figure 4: image converted into black and white pixels.

Virtual model generation (determination of optical and geometrical characteristics).

In a vector graphics editor software each of the curves corresponding to the empty areas of the tree were determined (figure 5). With this processing the virtual models were developed in CAD software, the curves were projected on a laminar semisphere for the perforated obstruction system (figure 6) and on a semisphere of multiple elements for the louvers system (figure 7).

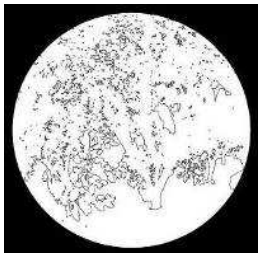

Figure 5: image of vectorized curves extracted from fisheye image.

Figure 6: projection and substraction of curves corresponding to the empty spaces for the perforated obstruction model (TracePro®).

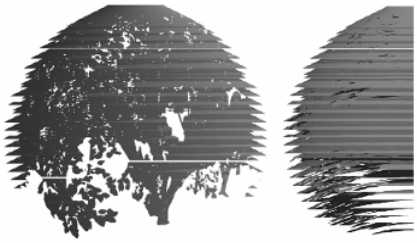

Figure 7: front and lateral view of the projection and substraction of curves corresponding to empty spaces for louvers model (TracePro®).

Figure 8: complete model: tree simplification, back vertical surface and horizontal inferior surface (TracePro®).

As previously mentioned, information regarding the general dimensional characteristics of the tree was collected for the virtual construction of the three models (Martínez, 2011): average height: 12.5 m (tree typology of second magnitude); average trunk perimeter at 1 meter height: 1.30 cm.

Besides the different representations of the tree as elements of solar control, other simplified urban elements were added. A vertical surface was used in the back part of the tree model to represent the white wall (flat white paint, 90% diffuse reflecting TracePro®) located in the site of study. A horizontal surface was added to represent the horizontal enclousure of the street (figure 8).

Direct illuminance for each hour in which the simulation would be carried out was measured in order to determine the characteristics of the incident light source (sun) (table 1). The obtained data was later employed to characterize the source.

Table 1
Direct solar illuminance values.

hour	Direct illuminace (klux)
10:30	109.17
11:30	112.43
12:30	114.23
13:30	116.45
14:30	114.23
15:30	112.43
16:30	109.17

The ray density employed for the simulation was based on the works of Andersen (2004), where she determines that for a 6cm diameter source, a 200000 ray density is sufficient. Proportionally, the amount of necessary rays was calculated for a 100 cm source, the required size for the surface of detection to be completely covered by the incident radiation. A 0.05 flux threshold was employed for ray extinction. It has been verified that a greater number of rays (500000) or a smaller flux threshold (0.001) do not significantly affect the results, both generated a difference inferior to 1% and significantly prolonged the simulation time (Andersen, 2004). The surface sources were located according to the altitude and azimuth corresponding to the sun position for each of the hours of simulation. Due to the fact that the sun behaves as a completely collimated source, a normal angular distribution was selected for the surface source.
Radiation coming from these surfaces source and incident on the detection surface will be called "global incident radiation" in this study in order to distinguish it from the "reflected incident radiation". The reflected incident radiation being that which radiates from the concrete horizontal surface, whose origin are also the surfaces source.

Specific considerations on the louvers model

For the development of the louver model, the predominant angle of inclination of tree leaves was determined, based on the Ryu protocol (2010). The analysis was carried out by taking a sample of 726 leaves corresponding to 20 mulberry specimens located in downtown Mendoza city. The obtained results establish that 60% of the leaves present a 15º to 45º inclination, with a mean of 31° 82' and a median of 30º 33` (figure 9). In order to simplify the model the 30º value was used.
Given previous studies (Martinez, 2011) it is known that the average longitudinal size of the mulberry leaf is 14.2cm, information which turned out to be crucial.

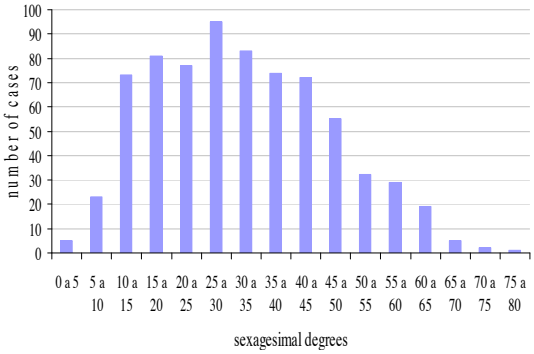

Figure 9: histogram: frequence of inclination angle of mulberry leaf in the selected specimens, every 10 º degrees.

Photos were taken to determine the inclination angle of the peripheral branches. Three-dimensional models were developed with these images in a CAD software, where the inclination angle of the branches was measures. An average of 40º degree inclination in relation to the horizontal surface was detected (figure 10).

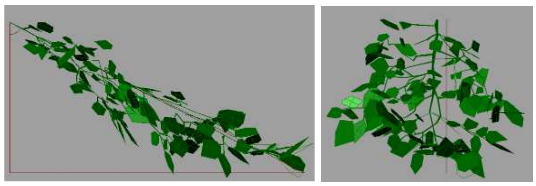

Figure 10: 3D models of the inclination angle of branches of the trees studied.

This set of geometrical considerations enabled the generation of the virtual model volumetry corresponding to the louvers system. A triangular grid was generated according to the inclination angle of leaves and branches which allowed to locate the “leaf element” in the outline of the circumference (figure 11 a and b). These elements were later extruded to conform the semisphere of light shelves.

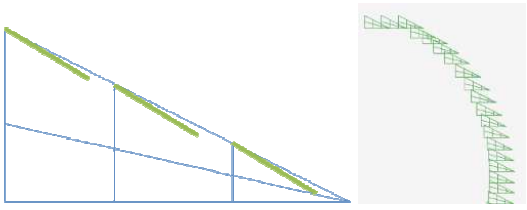

a *b*

Figure 11: distribution and inclination grid of leaves (a). Diagram of branches and leaves dispostion (b).

The distribution of the elements in the louvers model, following the branch diagram, produces successive filtrations of radiation (atenuation factor). This causes reductions in the transmitted light flux, therefore it is correct to use the normal transmittance of the material measured according to what figures 12 a and b indicate. This concept implies the consideration of sun radiation as a collimated, strongly directional source. The measurement of normal transmittance was carried out with an LMT photometer POCKET-LUX 2A with V lambda filter and cos-correction and a box with black interior, that was routed normally to the solar incidence, thus registering with and without the leaf element. From this analysis it was determined that the average transmittance of the mulberry leaf is 50%.

Figure 12: measurement diagram of transmittance without leaf (a) and with leaf (b).

Specific considerations on the perforated obstruction model and the homogenous transmittance model.

In both the perforated obstruction and the homogenous transmittance models, visible solar radiation filtrates only once, thus it is adequate for these models to use the standard transmittance established for leaves. Oke (1990) establishes that for the range of solar spectrum comprehended between 0.38 μm and 0.71μm the transmittance of a leaf is 6%.

Optical considerations common to the three models

The reflectance of leaves was determined according to the Fontoynont (1999) measurement protocol which allows to establish the hemispherical-hemispherical reflectance of lambertian materials. A Minolta LS 110 illuminance meter (1/3° acceptance angle and 0.01 to 999.900 cd/m2 accuracy) was used for this measurement, as well as pattern cards. The hemispherical-hemispherical reflectance obtained was 0.11 (1%).

In relation to the horizontal surface incorporated, optical properties corresponding to concrete were assigned. The performance of the different models was analyzed with the reflectance factor in relation to the incident angle of radiation (Table 2) (Ayuntamiento de Barcelona, 2012).

Table 2
Reflectance in relation to incident angle of radiation of concrete (Ayuntamiento de Barcelona, 2012).

50º	60º	70º	80º
0.151	0.153	0.155	0.157

This angular reflectance values of the concrete were summed for some of the scenarios with calculations (e.g. scenario A: louvers model, calculated reflected solar radiation) and for others directly inserted as data for the characterization of the material in the simulator (e.g. scenario B: louvers model, simulated reflected solar radiation).

Scenarios on which simulations were carried out.

Different scenarios were assigned according to the characteristics of the models:

A- louvers model, calculated reflected solar radiation
B- louvers model, simulated reflected solar radiation
C- perforated obstruction model, simulated reflected solar radiation
D- perforated obstruction model, calculated reflected solar radiation
E- homogenous transmittance model, simulated reflected solar radiation

Reference measurement

Vertical illuminance measurements over an eight point grid (50 cm diameter) were taken as the reference standard (radiometer ILT 1700 multiplexer A415 with an 8 channel selector for multiple detector input SCD110 Internacional Light), at first floor facade level (5m) (figure 13). The vertical illuminance values observed at facade level in the context of a forested street oscilate between 1000lux and 1600lux (figure 14), maximum at solar midday and minimum for the hours when solar altitude is lower. This type of tree reduces global daily vertical illuminance (between 77000lux and 23000 lux) in a significant way (between 96 and 98%) during the day.

In the virtual models the detection surface was placed on the rear vertical surface, according to its position on the facade in the measuring situation.

Figure 13: illuminance sensors located on the measurement grid.

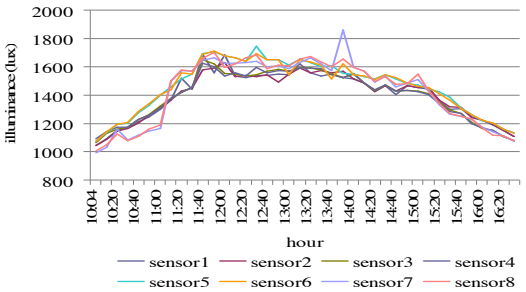

Figure 14: graphic of vertical illuminance values over facade on forested street registering each one of the 8 sensors in an range from 10.00 to 16.30.

The measurement was carried out on December 22nd corresponding to the summer solstice, period in which the tree presents significant leaf development. Sky condition for the day the measurement was performed was corroborated with global and diffuse

horizontal illuminance data of the Measurement Station INCIHUSA CCT-CONICET Mendoza (belonging to the International Network of Natural Lighting Measurement Stations IDMP) (figure 15).

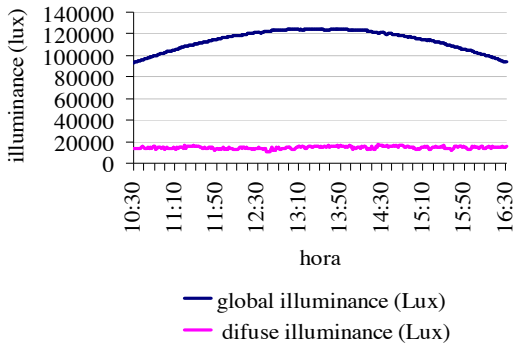

Figure 15: data of the sky condition for the day of measurement: global and diffuse hourly illuminance (lux) value.

Simulation

The simulations were perfomed with TracePro® software, a high precision simulator (figure 16 a, b and c). TracePro® is a ray tracing program for optical analysis of solid models, which uses a generalized ray tracing method. This technique allows you to launch rays into a model without making any assumptions as to the order in which objects and surfaces will be intersected. At each intersection, individual rays can be subject to absorption, reflection, refraction, diffraction and scatter. TracePro® uses the ray splitting model of Monte Carlo Simulation (TracePro® Manual, 2010).
Simulations were performed on a computer with the following general characteristics: CPU: Intel (R) Core (TM) i3-2100 3.10GHz; RAM 4.00 GB; 64-bit operating system; GPU: ATI Radean HD 5450. Process raytracing data and output is displayed in Table 3.

Table 3
Parameters of ray tracing simulation.

Analysis units	photometric
Flux threshold	0.05
Analysis output	Illuminance maps

The simulations were performed every hour from 10.30 to 16.30, which enables to analyze the degree of adjustment of the models to diferent angles of incidence of solar radiation, in accordance with the solar dynamics.

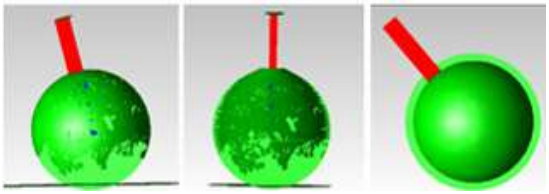

a *b* *c*

Figure 16: ray tracing for the perforated obstruction model TracePro® (a). Ray tracing for the louvers model TracePro® (b). Ray tracing for homogenous transmittance model TracePro® (c).

Statistical analysis of results

The statisticians employed to perform the comparison of the data sets are: root-mean-square error (RMSE) (1) and mean biased error (MBE) (2), their corresponding equations being:

$$RMSE=[\Sigma_i^n(E_m-E_s)^2/n] \,/\, [\Sigma_i^n E_m / n] \quad (1)$$

$$MBE=\Sigma_i^n(E_m-E_s) \,/\, \Sigma_i^n E_m / n \quad (2)$$

In which E_m indicates the average vertical illuminance values of the 8 points on the grid of measurement for each of the measured hours taken as reference, E_s corresponds to the average vertical illuminance values of the 8 points of the grid of simulation for each hour, n being the number of cases considered.
The RMSE allows to determine the difference between the measured and the simulated values.

DISCUSSION AND RESULT ANALYSIS

Table 4 indicates the average vertical illuminance values hourly and the RMSE and MBE for each of the studied scenarios.

Table 4
Measured and simulated vertical illuminances, RMSE and MBE.

	Vertical illuminance (lux)					
Hour	measure	**A**	**B**	**C**	**D**	**E**
10:30	*1157*	1194	523	938	1654	252
11:30	*1504*	1440	786	1017	1706	1412
12:30	*1621*	1812	1639	1987	2829	2199
13:30	*1592*	1706	1786	1663	2651	2508
14:30	*1504*	1635	1449	1472	2201	2199
15:30	*1311*	1463	903	2324	3220	1412
16:30	*1099*	1249	531	938	1313	252
Average	*1398*	1500	1088	1477	2225	1462
RMSE		**0.09**	**0.33**	**0.33**	**0.72**	**0.48**
MBE		**-0.07**	**0.17**	**-0.23**	**-0.10**	**0.49**

The louvers model with calculated reflected visible solar radiation presents an RMSE of 0.09, while the louvers model with simulated reflected visible solar

radiation shows and RMSE of 0.33. The results that the RMSE show are clearly observed in figure 17, where the similarity in behavior presented by scenario A in relation to the measured values can be percieved, differences in average lower than 120 lux. For scenario B the hours corresponding to lower incidence angles (morning and afternoon) present values significantly distant from the measured, an average difference of 500 lux. This error resulting from the deficiency of the louvers model to determine by means of simulation the incident radiation over the facade as a result of the reflection of the concrete. This is due to the successive reductions of radiation applied by the model, given its geometrical disposition. In addition, the data available for the characterization of concrete does not correspond with a complete bidirectional transmittance-reflectance base, which precludes the characterization of the material as a lambertian surface.

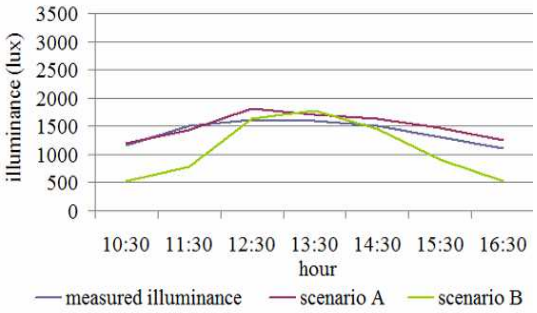

Figure 17: hourly illuminance values from 10.30 to 16.30 for the measure reference and the louver models (scenario A and B).

As for the perforated obstruction models an RMSE of 0.33 was obtained for the scenario of simulated reflected solar radiation (C) and an RMSE of 0.72 for the situation of calculated reflected visible solar radiation (D). These results clearly indicate that this model responds better to simulated reflected solar radiation (scenario C) (figure 18), due to its low capacity of atenuation of incident visible solar radiation. However, model C presents difficulties for the calculation of reflected radiation in situations in which its own geometry reduces incident radiation over the horizontal surface (concrete) which later generates reflected solar radiation. Therefore with a detection threshold of 0.05 the reflected radiation is depreciated. If the detection threshold increases (0.005) the reflected radiation can be detected, however, the direct vertical illuminance values increase significantly. Besides, the simulation time is three times longer with respect to the same scenario with a 0.05 detection flux threshold.

The high vertical illuminance values detected represent the most significant misalignments of the perforated obstrution model. This is due to luminous fluxes passing through the perforations (transmittance 1), which generates highly elevated illuminance areas, since it is direct solar radiation. It seems that this is due to the limited ability presented by this model to reproduce successive reflection and transmittance interactions produced in the real context between the different elements of the canopy. Analysis of vertical illuminance measurement over the facade on a forested street shows that there is no incidente direct solar radiation over the detection grid. In figures 19 a and b is displayed clearly the above situation.

If we compare these results to the louvers model, we can see that the perforated obstruction scenario with a better response (C) shows a similar root-mean-square error close to the louvers scenario that presents lower adjustment (B).

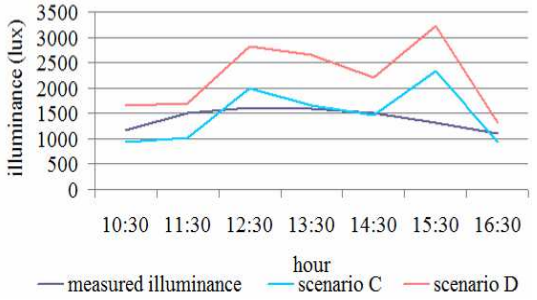

Figure 18: hourly illuminance values from 10.30 to 16.30 for the reference measure and perforated obstruction models.

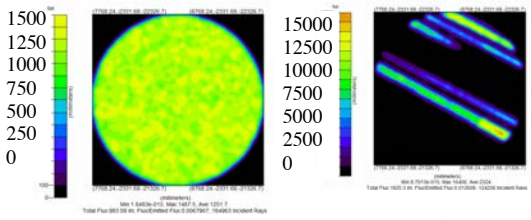

a *b*

Figure 19: distribution of illuminances for the perforated obstruction models when direct vertical solar radiation strikes (a) (TracePro®) and when it does strike (b) (TracePro®).

The model of homogenous transmittance (E) shows a high RMSE value (0.48) (figure 20), this situation is due to the lack of treatment from the bidirectional perspective of the system's transmittance. This model rejects the reflected component for all the positions of the source since the incident radiation is filtered by the semisphere (6% transmittance) in the incoming and outgoing, resulting radiation available to be reflected by the horizontal surface lower than 5%.

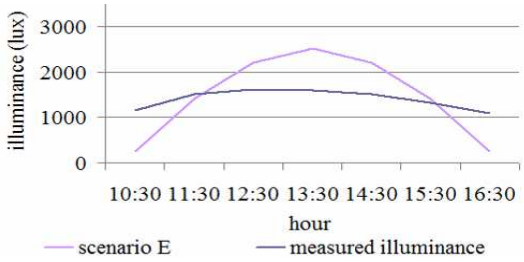

Figure 20: hourly illuminance values from 10.30 to 16.30 for reference measure and homogenous transmittance model.

Concerning the simulation time (with a Intel (R) Core (TM) i3-2100 3.10GHz processor), the homogenous transmittance model is observed to present the longest simulation time (approximately 47 minutes), this appears to be due to the non faceted geometrical disposition. On the other hand, although the perforated obstruction model takes less time of execution, this model adjusts better when both components -global and reflected radiation- are obtained by simulation, while for the louvers model with calculated reflected radaition the time is even shorter since only the global simulation must be effected (Table 5).

In a more detailed way we observe, the number of components presented in the models are representatively different, this is displayed in the times of the revision of the entity properties and the preparation of the geometry processes (Table 5).

Table 5
*Simulation time: 1 Revision of the entity properties, 2 Preparation of geometry, 3 Ray tracing process. *B and C scenario only simulation time of global solar radiation should be considered.*

Model		Nº elements	time (seconds)				
			1	**2**	**3**	total parcial	total
A-B*	Glo	646	45	15	745	805	1536
	Ref		35	11	685	731	
C-D*	Glo	40	0	10	344	354	1006
	Ref		0	14	638	652	
E	Glo	3	0	0	1397	1397	2860
	Ref		0	0	1463	1463	

CONCLUSIONS

The degree of adjustment of the three models based on solar control systems was verified in relation to the behavior of the public urban forest with respect to visible solar radiation. The methodology employed is based on hemispherical images and raytracing simulation, validating the simulation results with measurements in situ of vertical illuminance values. The deficiencies of each virtual model in the reproduction of reality were analyzed, given the high complexity presented by the studied element. The louvers model with calculated reflection (scenario A) shows a higher degree of adjustment (9% error) in relation to the measured data, since this model shows a higher capacity to interact with radiation through interreflections and diverse moments of light filtering, given its disposition and physical properties. This scenario becomes even more usefull if the limited simulation time demanded is considered in relation to the other scenarios.

Models that base their performance primarily in transmittance phenomenon, need to be approached from a bidirectional perspective, since they do not have the capacity to interact with incident radiation beyond transmittance. In further studies approaches to bidirectional transmittance for perforated obstruction and homogenous transmittance models will be carried out.

NOMENCLATURE

E_m: average vertical illuminance for each of the measured hours taken as reference.

E_s: average vertical illuminance for each of the simulated hours.

n: number of cases considered.

ACKNOWLEDGEMENT

The authors wish to thank Dr. Raúl Ajmat for his enlightening advice in simulation assessments.

Authors thank Lambda Research Corporation for concession of the TracePro® Software license used for the studies related to the Doctoral Thesis MAVILE, Faculty of Sciences and Technology, National University of Tucumán, with doctoral CONICET scholarship of the student Ayelén Villalba.

Authors also wish to thank Dr. Lorena Corica, Juan Manuel Monteoliva and Juan Pablo Calire.

REFERENCES

Al-sallal, K., Ahmed, L. 2007. Improving natural light in classroom spaces with local trees: Simulation analysis under the desert conditions of the uae. Proceedings: Building simulation, Ninth international IBPSA conference, Beijing, China, pp. 1168- 1174.

Al-sallal, K. 2009. Practical method to model trees for daylighting simulation. Using hemispherical photography. Proceedings: Building simulation. Eleventh international IBPSA conference, Glasgow, Scotland, pp. 280-285.

Andersen, M. 2004. Innovative Bidirectional Video-Goniophotometer for Advanced Fenestration Systems. PhD Tesis.Swiss Federal Institute of Technology, Solar Energy and Building Physics Laboratory, Switzerland.

Baker, N., Fanchiotti A., Steemers K (eds). 1993. *Daylighting in Architecture A European Reference Book*, James & James, London, UK.

Blennow, K. 1995. Sky view factors from high resolution scanned fish-eye lens photographic negatives. *Journal of Atmospheric and Oceanic Technology*, 12, pp1357-1362.

Campbell G.S., Norman J.M. 1989. The description and measurement of plant canopy structure, in: Russell G., Marshall B., Jarvis P. G. (Eds.), *Plant canopies: their growth, form and function*, Cambridge University Press, pp. 1-19.

Coder, R. D. 1996. Identified Benefits of Community Trees and Forests. University of Georgia.

Correa, E. N., et al. 2005. Evaluación del factor de visión de cielo a partir del procesamiento digital de imágenes hemisféricas. Influencia de la configuración del cañón urbano en la disponibilidad del recurso solar. *Avances en energías renovables y medio ambiente*, 9(11), pp. 43-48.

Correa, E. N., Ruiz, M. A., Cantón, A. 2010. Morfología forestal y confort térmico en "ciudades oasis" de zonas áridas. *Ambiente Construído*, 10 (4), pp. 119-137.

Correa, E. N., et al. 2012. Thermal comfort in forested urban canyons of low building density. An assessment for the city of mendoza. *Building and environment*, 58, pp. 219-230.

Córica, L. 2009. Comportamiento de la luz natural en entornos urbanos representativos del modelo oasis en regiones áridas. Caso de estudio: ciudad de Mendoza. PhD Thesis, Faculty of Sciences and Technology, National University of Tucumán. PhD: 299.

Fontoynont M. 1999. *Daylight performance of buildings*. ENTPE, Lyon.

Getz, D. A., Karow, A., Kielbaso, J. J., 1982. Inner city preferences for trees and urban forestry programs. *Journal of arboricultura*, 8(10), 258-263.

Martinez, C. F. 2011. Incidencia del déficit hídrico en forestales de ciudades oasis: caso del Área Metropolitana de Mendoza, Argentina. PhD Thesis. Biology Postgraduate PROBIOL, Cuyo National University.

Oke, T., R. 1990. Boundary layer climates. 2ª ed. Routledge, London.

Reflectancias suelos urbanos. Ayto. de Barcelona. www.terra.es/personal6/a.fontm/reflec.htm

Rodríguez, R. G. 2012. Análisis de estresores visuales y cognitivos en trabajo de oficina con PVD. El caso de las TIC. PhD Thesis, Faculty of Sciences and Technology, National University of Tucumán. PhD: 201.

Ryu, Y., et al. 2010. How to quantify tree leaf área index in an open savannas ecosystem: A multi-instrument and multi-model approach. *Agricultural and Forest Meteorology*. 150, pp. 63-76.

Santamouris, M. et al. 2001. Energy and climate in the urban built environment. London: James & James.

TracePro® User´s Manual. 2010. Lambda Research Corporation, Littleton, MA.

Villalba, A., Pattini, A., Córica, L. 2011. Análisis de las características morfológicas de las envolventes edilicias y del entorno urbano desde la perspectiva de la iluminación natural. *Ambiente Construido*, 12(4), pp. 159-175.